Is a large mixing angle MSW effect the solution of the solar neutrino problems?

J. N. Bahcall
School of Natural Sciences, Institute for Advanced Study, Princeton, New Jersey 08540

P. I. Krastev
University of Wisconsin–Madison, Department of Physics, Madison, Wisconsin 53706

A. Yu. Smirnov
International Center for Theoretical Physics, 34100 Trieste, Italy
(Received 6 May 1999; published 4 October 1999)

Recent results on solar neutrinos provide hints that the LMA MSW solution could be correct. We perform accurate calculations for potential ''smoking-gun'' effects of the LMA solution in the SuperKamiokande solar neutrino experiment, including (1) an almost constant reduction of the standard recoil electron energy spectrum (with a weak, $<10\%$, relative increase below 6.5 MeV), (2) an integrated difference in day-night rates (2%–14%), (3) an approximately constant zenith-angle dependence of the nighttime event rate, (4) a new test for the difference in the shape of the equally normalized day-night energy spectra ($\sim 1\%$), and (5) annual variations of the signal due to the regeneration effect (~ 6 times smaller than the integrated day-night effect). We also establish a relation between the integrated day-night asymmetry and the seasonal asymmetry due to LMA regeneration. As a cautionary example, we simulate the effect of an absolute energy calibration error on the shape (distortion) of the recoil energy spectrum. We compare LMA predictions with the available SuperKamiokande data for 708 days of operation and discuss the possibilities for distinguishing experimentally between LMA and vacuum oscillations. If LMA is correct, global solutions combining data from different types of measurements made by SuperKamiokande or by different solar neutrino experiments could reveal in the next few years a many σ indication of neutrino oscillations. [S0556-2821(99)07919-9]

PACS number(s): 14.60.Pq, 12.15.Ff, 26.65.+t, 96.60.Jw

I. INTRODUCTION

On 1 April 1996, solar neutrino research shifted from the pioneering phase of the chlorine (Homestake) experiment [1] and the exploratory phase of the Kamiokande [2], SAGE [3], and GALLEX [4] experiments to the era of precision measurements inaugurated by the SuperKamiokande [5–11] experiment. In this paper, we concentrate on the predictions for ''smoking-gun'' evidence of new neutrino physics that can be observed in electron-neutrino scattering experiments such as SuperKamiokande.

There are four generic oscillation solutions [large mixing angle (LMA), small mixing angle (SMA), and low mass-squared difference and/or low probability (LOW) Mikheyev-Smirnou-Wolfenstein (MSW) solutions and vacuum oscillations; cf. Ref. [12] for a recent discussion] of the solar neutrino problems that involve two neutrinos. These solutions are all consistent with the predictions of the standard solar model [13] and the observed average event rates in the chlorine, Kamiokande, SuperKamiokande, GALLEX, and SAGE experiments. We limit ourselves to such globally consistent oscillation solutions and adopt the methodology used in our recent paper [12].

Recent experimental results from SuperKamiokande [6–9] provide some encouragement for considering the LMA solution of the MSW effect [14]. No statistically significant distortion of the recoil electron energy spectrum has been discovered. No obvious change has been revealed in the slope of the ratio [measurement/(standard spectrum)] as the SuperKamiokande measurements have been extended to progressively lower energies. Moreover, the excess of events at the highest energies has diminished.

A larger flux has been observed at night than during the day, although the difference observed by SuperKamiokande [6–9] (which is about the size of what is expected from the LMA solution) is only $\sim 1.6\sigma$ after 708 days of data collection [15]. In addition, no large enhancement of the rate has been found when the neutrino trajectories cross the Earth's core. Moreover, the excess that is found appears already when the Sun is just below the horizon. These results are, as we shall see in detail in this paper, expected on the basis of the LMA MSW solution but are not expected on the basis of the SMA solution.

There are also some non-solar indications that large mixing angles may be plausible. First, and most important, SuperKamiokande and other experiments on atmospheric neutrinos have provided strong evidence that large lepton mixing is occurring at least in one channel involving muon neutrinos [16]. Moreover, the mass required for the LMA solution [$m \sim \sqrt{(\Delta m^2)} \sim 10^{-2}$ eV] is only one order of magnitude smaller than the mass scale suggested by atmospheric neutrino oscillations. All of the other solar neutrino solutions imply a smaller or much smaller neutrino mass scale for solar neutrinos. It is however well known that a weak mass hierarchy allows a rather natural explanation of large mixing.

The oscillation parameters of the LMA solar neutrino solution can give an observable effect for atmospheric neutrino experiments. In particular, the LMA solution could explain [17] the excess of *e*-like events in the atmospheric data.

In this paper, we provide accurate calculations for smoking-gun predictions of the LMA solution, including a simple new test (Sec. III C). In particular, we calculate and compare with SuperKamiokande observations the following

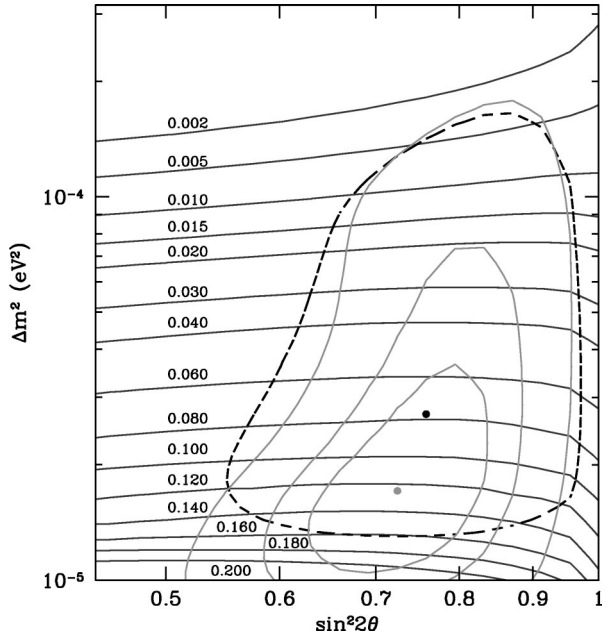

FIG. 1. The allowed region of the LMA MSW parameter space. When only the rates in the chlorine, SuperKamiokande, SAGE, and GALLEX experiments are considered, the largely-vertical solid lines are the allowed contours at 90%, 95%, and 99% C.L. The dashed contour corresponds to the allowed region at 99% C.L. when both the total rates and the night-day asymmetry are included. The best fit parameters, indicated by a dot in the figure, are for the rates-only fit: $\sin^2(2\theta)=0.72$ and $\Delta m^2=1.7\times10^{-5}$ eV^2. The best-fit parameters for the combined fit are $\sin^2(2\theta)=0.76$ and $\Delta m^2=2.7\times10^{-5}$ eV^2. The approximately horizontal lines show the contours for different night-day asymmetries (numerical values indicated); see Ref. [30] for an illuminating discussion of the night-day asymmetry. The data are from Refs. [1,3,4,9].

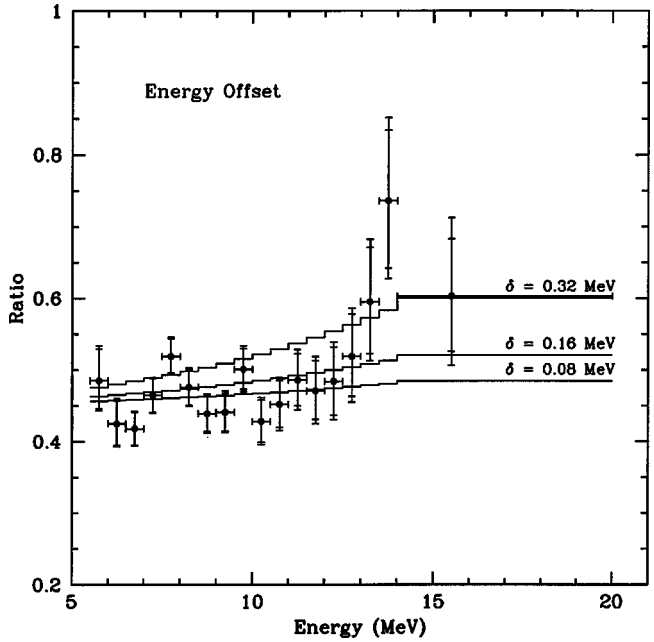

FIG. 2. The effect of a hypothetical energy calibration error on the shape of the electron recoil energy spectrum. The data points represent 708 days of SuperKamiokande observations [9]. The three curves were calculated from Eq. (3) for constant values of the energy offset parameter, δ, of 80 keV, 160 keV, and 320 keV. For visual convenience, each curve was calculated with a somewhat different normalization.

quantities: (1) the distortion of the electron recoil energy spectrum, (2) the zenith angle dependence of the observed counting rate, (3) the day-night spectrum test, and (4) the seasonal dependence (beyond the effect of the Earth's eccentric orbit) of the counting rate. All of these quantities are zero, independent of solar physics, if the standard model for electroweak interactions is correct. Therefore, measurements of the spectral energy distortion and the zenith angle and seasonal dependences constitute sensitive smoking-gun tests of new physics. As a cautionary example, we also simulate the effect of an energy calibration error on the apparent distortion of the electron recoil energy spectrum.

Figure 1 shows the allowed region of LMA solution in the plane of $\sin^2 2\theta$ and Δm^2. We have indicated the region allowed by the measured total rates in solar neutrino experiments by the continuous contours in Fig. 1; the contours are shown at 90%, 95%, and 99% C.L. The constraints provided by the the total rates in the Homestake, GALLEX, SAGE, and SuperKamiokande experiments are, at present, the most robust limitations on the allowed parameter space. The only slight change in the available data on total rates since the publication of Ref. [12] is a small reduction after 708 days in the total error for the SuperKamiokande experiment [9]; the allowed region based upon the total rates in solar neutrino experiments is essentially unchanged from our earlier study (cf. the similar results in Fig. 2 of Ref. [12] for the case that only the total rates are considered).

The dashed line in Fig. 1 represents the 99% allowed contour including both the measured SuperKamiokande day-night effect and the total rates. The SuperKamiokande Collaboration has performed preliminary global analyses of the available 708 days of data [9,10,15] .

Table I contrasts the predictions of the standard model and the LMA for the chlorine and the gallium experiments. The LMA results that are not in parentheses are for $\Delta m^2=2\times10^{-5}$ eV^2 and $\sin^2 2\theta=0.8$. These neutrino parameters are close to the best-fit LMA values when only the total rates of the chlorine, Kamiokande, SuperKamiokande, GALLEX, and SAGE experiments are considered (see Ref. [12]). In parentheses, we show the predictions for two rather extreme LMA solutions. We have evaluated the predictions for the chlorine and gallium experiments for a representative set of oscillation parameters and all of the values lie within the boundaries defined by the three solutions shown in Table I. Therefore, the predictions given in the table show the expected range of capture rates consistent with the LMA solution and the existing experiments. The range of production rates predicted by the set of LMA oscillation solutions considered in this paper is $^{37}\mathrm{Cl}=2.9\pm0.3$ SNU and $^{71}\mathrm{Ga}=71\pm9$ SNU.

The prediction of the LMA solution shown in Table I for the SuperKamiokande rate due to the ^{8}B neutrino flux [5,6,8,9] is rate (measured, ^{8}B)$=0.474$ rate (BP98, ^{8}B).

This paper is organized as follows. We discuss the distortion of the recoil electron energy spectrum in Sec. II, the

TABLE I. Standard solar model and LMA predictions for solar neutrino rates. The standard solar model predictions are taken from BP98 [13]. The LMA predictions refer to the best-fit LMA solution when only the total rates are considered: $\Delta m^2 = 2\times10^{-5}$ eV^2 and $\sin^2 2\theta = 0.8$ (cf. Ref. [12]). (The values given in parentheses were computed using, respectively, the oscillation parameters $\Delta m^2 = 8\times10^{-5}$ eV^2, $\sin^2 2\theta = 0.63$ and $\Delta m^2 = 8\times10^{-5}$ eV^2, $\sin^2\theta = 0.91$.) The rates calculated using the BP98 fluxes and the LMA oscillation solution agree with the measured rates for the Homestake chlorine experiment (2.56 ± 0.23 SNU; see Ref. [1]) and the SAGE (67 ± 8 SNU; see Ref. [3]) and GALLEX (78 ± 6 SNU; see Ref. [4]) gallium experiments.

Source	Flux	Cl (SNU)	Ga (SNU)	Cl (SNU)	Ga (SNU)
	Standard	Standard	Standard	LMA	LMA
pp	5.94	0.0	69.6	0.0 (0.0,0.0)	39.8 (47.1,37.5)
pep	1.39×10^{-2}	0.2	2.8	0.1 (0.1,0.1)	1.2 (1.8,1.4)
hep	2.10×10^{-7}	0.0	0.0	0.0 (0.0,0.0)	0.0 (0.0,0.0)
^{7}Be	4.80×10^{-1}	1.15	34.4	0.46 (0.65,0.60)	15.7 (21.5,17.4)
^{8}B	5.15×10^{-4}	5.9	12.4	1.8 (1.6,2.3)	3.7 (3.4,4.8)
^{13}N	6.05×10^{-2}	0.1	3.7	0.05 (0.06,0.05)	1.8 (2.4,1.9)
^{15}O	5.32×10^{-2}	0.4	6.0	0.16 (0.25,0.20)	2.5 (3.8,3.1)
Total		$7.7^{+1.2}_{-1.0}$	129^{+8}_{-6}	2.6 (2.65,3.2)	64.7 (80,66)

[a]All fluxes are in units of (10^{10} cm^{-2}s^{-1}).

day-night differences of the event rate in Sec. III, and the seasonal dependences in Sec. IV. We describe in Sec. V possibilities for distinguishing between LMA and vacuum oscillations. We summarize and discuss our main results in Sec. VI.

II. SPECTRUM DISTORTION

Figures 2 and 3 illustrate the main results of this section. The reader who wants to get quickly the essence of the physical situation can skip directly to the discussion of Fig. 2 in Sec. II C and Fig. 3 in Sec. II D.

The observation of a distortion in the recoil electron energy spectrum produced by solar neutrinos scattering off electrons would be a definitive signature of physics beyond the standard electroweak model. Neutrinos which correspond to recoil electrons with energies between 5 MeV and 13 MeV, which are most easily observed by the SuperKamiokande solar neutrino experiment [5,6,8,9], are predicted by the standard solar model to be essentially all (more than 99%) from ^{8}B beta decay [13]. The shape of the ^{8}B neutrino energy spectrum can be determined accurately from laboratory measurements [18] and the influence of astrophysical factors is less than 1 part in 10^5 [19]. For energies relevant to solar neutrino studies, the cross sections for neutrino scattering have been calculated accurately in the standard electroweak model, including radiative corrections [20]. Therefore, if nothing happens to solar neutrinos on the way from the region of production in the solar interior to a detector on Earth, the recoil electron energy spectrum from ^{8}B neutrinos can be calculated precisely.

Any measured deviation of the recoil electron energy spectrum from the standard shape would indicate new physics. The opposite, however, is not true: the absence of a measured distortion does not mean the absence of new physics.

We first indicate in Sec. II A how the neutrino energy

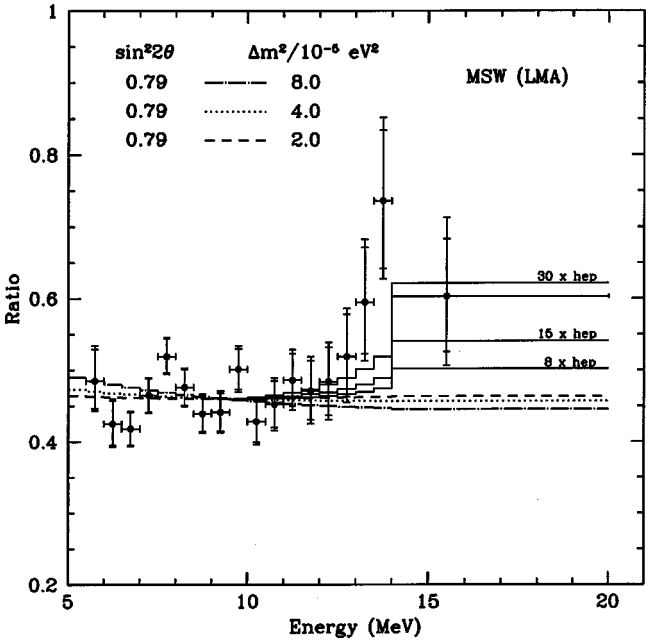

FIG. 3. Distortion of the ^{8}B electron recoil electron spectrum for large mixing angle MSW oscillations. The figure shows the ratio, R, of the measured number of electrons to the number expected on the basis of the standard model [13] [see Eq. (1)]. Solutions are shown with the standard model fluxes of ^{8}B and *hep* neutrinos (the approximately horizontal lines) and with the standard *hep* flux multiplied (see Ref. [21]) by factors of 8, 15, and 30 (ratio increases at highest energies). The calculated ratios are shown for three different values of Δm^2 and with $\sin^2 2\theta = 0.79$ in order to illustrate the range of behaviors that result from choosing neutrino parameters. Results similar to Fig. 3 are obtained if $\sin^2 2\theta$ is allowed to vary over a representative range of the allowed global LMA solutions that are consistent with the average measured event rates. The experimental points show the SuperKamiokande results for 708 days of observations [9].

spectrum is convolved with the electron recoil energy spectrum and with the measurement characteristics of the detector. We then summarize briefly in Sec. II B the characteristics of the measured SuperKamiokande energy spectrum. In Sec. II C, we answer the question: How does an error in the energy calibration affect the shape of the recoil energy spectrum? We discuss in Sec. II D the comparison of the predicted and the measured electron energy spectra, which are presented in Fig. 3.

A. Convolution

We concentrate in this paper on analyzing the ratio, $R(E_i)$, of the number of observed events, $N_i^{\rm Obs}$ in a given energy bin, E_i, to the number, $N_i^{\rm SSM}$, expected from the SSM [13], where

$$R(E_i)=\frac{N_i^{\rm Obs}}{N_i^{\rm SSM}}. \tag{1}$$

For specific applications, we use the observed event numbers in the form provided by SuperKamiokande [8,9]; there are 17 energy bins of 0.5 MeV width from 5.5 MeV to 14 MeV and an 18th bin that includes all events from 14 MeV to 20 MeV. When more data are available, it will be important to divide the events above 14 MeV into several different bins [21].

The number of events in a given energy bin, *i*, can be expressed as

$$N_i=\int_{E_i}^{E_i+0.5MeV}dE_e\int_0^\infty dE_e' f(E_e,E_e')\int_{E_e'}^\infty dE_\nu F(E_\nu) \times\left[P(E_\nu)\frac{d\sigma_e(E_\nu,E_e')}{dE_e'}+[1-P(E_\nu)]\frac{d\sigma_\mu(E_\nu,E_e')}{dE_e'}\right], \tag{2}$$

where $F(E_\nu)$ is the flux of ^{8}B neutrinos per unit energy at the detector, and $f(E_e,E_e')$ is the energy resolution function which we take from [5,6]. $P(E_\nu)$ is the survival probability $\nu_e\rightarrow\nu_e$, $d\sigma_e/dE_e'$ and $d\sigma_\mu/dE_e'$ are the differential cross sections of the $\nu_e e$ and $\nu_\mu e$ scattering. There are practically no ^{8}B neutrinos with energies greater than 15.5 MeV, so that for practical purposes the upper limit of the integral over E_ν in Eq. (2) can be taken to be 16 MeV. Including the effects of the finite energy resolution, the upper limit over the measured electron recoil energy, E_e', can be taken to be 20 MeV.

To use Eq. (2) to calculate the combined prediction for the standard electroweak model and the standard solar model, set $P\equiv 1$. The second term in the brackets of Eq. (2) then disappears. This term is also absent if the electron neutrinos are converted to sterile neutrinos.

How does the convolution shown in Eq. (2) affect energy-dependent distortions (or conversions) of the incoming electron neutrinos? The convolution spreads out over a relatively wide energy range any energy-dependent features. In particular, the scattering process produces electrons with energies from zero to almost equal to the incoming neutrino energy (for neutrino energies much greater than the electron mass). If ν_e are converted to ν_μ or/and ν_τ, then there will be neutral current scattering [the second term in the square brackets of Eq. (2)] which, while less probable, will also reduce the apparent effect of the conversion. Since the solar ^{8}B neutrino spectrum decreases rapidly beyond about 10 MeV, a distortion of the recoil electron spectrum at some energy E_e($E_e>10$ MeV) is determined by the distortion of the neutrino spectrum at somewhat lower energy $E_\nu<E_e$. The energy resolution function has a crucial affect in smearing out distortion. The 2σ width for the energy resolution is about 3 MeV at $E_e=10$ MeV in SuperKamiokande [5,6,8]. Smaller features will be smeared out.

B. Summary of the data

After 708 days of data taking with SuperKamiokande, no unequivocal distortion of the electron recoil energy spectrum has been found. The data show essentially the spectrum shape expected for no distortion for $E<13$ MeV with some excess events at $E>13$ MeV. The excess electrons observed at higher energies may reflect (1) a statistical fluctuation, (2) the contribution of *hep* neutrinos [21–23], (3) a larger-than-expected error in the absolute energy normalization; or (4) new physics. The systematic effects due to *hep* neutrinos or to an error in the energy normalization can hide a distortion due to neutrino conversion or cause an artificial distortion. For example, a suppression due to oscillations of the high energy part of the electron spectrum could be compensated for (hidden by) the effect of *hep* neutrinos.

All of the four explanations for the high-energy excess have been described previously in the literature. However, the distortion due to an error in the absolute energy scale of the electrons has only been mentioned as a possibility [24]. Therefore, we discuss in Sec. II C the effect on the energy spectrum of an error in the absolute energy scale.

Another possible systematic error, a non-Gaussian tail to the energy resolution, could also produce an apparent distortion at the highest energies. However, this effect has been estimated by the SuperKamiokande Collaboration and found to be small [25,9].

To resolve the ambiguity at high recoil electron energies, one can proceed in at least two different ways. (1) One can exclude the spectral data above 13 MeV, since the distortion due to both *hep* neutrinos and the calibration of the energy scale normalization occur mainly at high energies. A comparison of the results of the analysis using all the data with the inferences reached using only data below 13 MeV provides an estimate of the possible influence of systematic uncertainties. However, this procedure does throw away some important data. (2) One can treat the solar *hep* neutrino flux as a free parameter in analyzing the energy spectrum [21,22]. In general, this is the preferred method of analysis and the one which we follow.

C. How does an energy calibration error affect the recoil energy spectrum?

An error in the absolute normalization of the energy of the recoil electrons, $\delta=E_{\rm true}-E_{\rm measured}$, would lead to an appar-

ent energy dependence in R that is particularly important for the LMA solution, since the theoretical prediction is that R is essentially constant in the higher energy region accessible to SuperKamiokande. The ratio $R(E)$ can be written as

$$R^{\mathrm{Obs}}(E)=\frac{N^{\mathrm{Obs}}(E+\delta)}{N^{\mathrm{SM}}(E)} \approx R_0^{\mathrm{true}}(E)\left(1+\frac{1}{N^{\mathrm{SM}}(E)}\frac{dN^{\mathrm{SM}}(E)}{dE}\delta\right), \qquad (3)$$

where $N^{\mathrm{SM}}(E)$ is the standard model spectrum. Since N^{SM}, dN^{SM}/dE and, in general, δ all depend on energy, the last term in Eq. (3) gives rise to an apparent distortion of the observable spectrum. Moreover, since $N^{\mathrm{SM}}(E)$ is a decreasing function of energy, $\delta\times(dN^{\mathrm{SM}}/dE)/N^{\mathrm{SM}}$ increases with energy for negative δ. Thus, for negative δ, $R(E)$ is enhanced at high energies. The SuperKamiokande collaboration has estimated the error in the absolute energy calibration as being 0.8% at 10 MeV [8], i.e., $\delta=80$ keV, 1σ.

We have simulated the effect of an error in the absolute energy calibration by convolving a standard model recoil energy spectrum with the energy resolution function of SuperKamiokande and introducing a constant offset error δ. We calculated the ratio $R(E)$ directly from the equality in Eq. (3), without making the approximation involved in the Taylor-series expansion.

Figure 2 compares the computed $R(E)$ for three different values of δ with the observed SuperKamiokande data [9] for 708 days. For visual convenience, each curve is normalized somewhat differently, but all are normalized within the range allowed by the SuperKamiokande measurement of the total rate. We see from Fig. 2 that a 2σ (160 keV) energy calibration error can produce a significant pseudo-slope. More exotic effects can be produced if the one assumes that the energy error, δ, is itself a function of energy.

We conclude that future analyses of the distortion of the energy spectrum should include δ as one of the parameters that is allowed to vary in determining from the measurements the best-fit and the uncertainty in the energy distortion.

D. Predicted versus measured spectra

Figure 3 compares the predicted versus the measured ratio $R(E)$ [see Eq. (1)] of the electron recoil energy spectra for a representative range of Δm^2 that spans the domain permitted by the global LMA solutions. All of the solutions shown have $\sin^2 2\theta=0.8$ and are consistent with the average event rates in the chlorine, Kamiokande, SAGE, GALLEX, and SuperKamiokande experiments. Also, all of the histograms of neutrino solutions are normalized so as to yield the same value of the ratio $R(E)$ at $E=10$ MeV. The measured values are taken from [9].

The most conspicuous feature of Fig. 3 is the flatness of the ratio $R(E)$ that is predicted by the LMA solution with no enhancement of the *hep* flux. The survival probability, P, without Earth regeneration is $P(E)\approx\sin^2\theta$ in the observable high energy part of the ^{8}B neutrino spectrum. Regeneration in the Earth can lead to a weak increase of the survival probability with energy.

TABLE II. Day-night asymmetries.

Δm^2 (10^{-5} eV^2)	$A_{\mathrm{n\text{-}d}}$ $\sin^2 2\theta=0.9$	$A_{\mathrm{n\text{-}d}}$ $\sin^2 2\theta=0.8$	$A_{\mathrm{n\text{-}d}}$ $\sin^2 2\theta=0.7$
8	0.019	0.018	0.017
4	0.049	0.050	0.049
3	0.069	0.073	0.071
2	0.100	0.107	0.107
1.6	0.126	0.135	0.136

Excellent fits to the recoil energy spectra can be obtained by increasing the production cross section for the *hep* flux by a factor of 10–40 over its nominal (see Ref. [26]) best value. This result is illustrated in Fig. 3.

Results similar to Fig. 3 are obtained if $\sin^2 2\theta$ is allowed to vary over a representative range of the allowed global LMA solutions that are consistent with the average measured event rates. We find numerically that the dependence of the shape of the predicted spectrum upon $\sin^2 2\theta$ is very weak.

Recent work by the SuperKamiokande Collaboration has placed an experimental upper limit on the *hep* neutrino flux at Earth of at most 20 times the nominal standard value [6,9,10]. The fits shown in Fig. 3 demonstrate that we require a *hep* flux at the sun of 10–40 times the standard value. However, LMA neutrino oscillations reduce the rate at the Earth so that the observed rate is about a factor of 2 less than would correspond to a flux of purely ν_e *hep* neutrinos. So the fits shown for variable *hep* flux in Fig. 3 are consistent with the SuperKamiokande upper limit on the measured *hep* flux.

What are the chances that SuperKamiokande can obtain smoking-gun evidence for a distortion of the energy spectrum if the LMA solution is correct? The lack of knowledge of the *hep* production cross section prevents fundamental conclusions based upon the suggestive higher energy ($>$13 MeV) events. The data reported by SuperKamiokande (at the time this paper is being written) above 14 MeV are in a single bin (14–20 MeV). As emphasized in Ref. [21], it is possible that measurements in smaller energy bins above 14 MeV could reduce the uncertainty in the *hep* flux and test the consistency of the LMA plus enhanced *hep* predictions (for preliminary results see Ref. [9]).

For larger allowed values of Δm^2, the distortion curve turns up at low energies (cf. Fig. 3). This upturn is due to the fact that for larger Δm^2 the low energy part of the ^{8}B neutrino spectrum ($E\sim 5$–6 MeV) is on the adiabatic edge of the suppression pit. For the smallest allowed Δm^2, LMA predicts a weak positive slope for $R(E)$ that is caused by the Earth regeneration effect.

The predicted distortion at low energies, between, e.g., 5 MeV and 6.5 MeV, is small (typically $\sim$ a few percent up to as large as 10%; cf. Fig. 3) and would require approximately 10 years of SuperKamiokande data in order to show up in a clear way.

III. EARTH REGENERATION EFFECTS

If MSW conversions occur, the Sun is predicted to be brighter at night in neutrinos than it is during the day [27] at

those energies at which the survival probability of ν_e is less than one-half. This phenomenon, if observed, would be a dramatic smoking-gun indication of new physics independent of solar models.[1]

When the Sun is below the horizon, neutrinos must traverse part of the Earth in order to reach the detector. By interacting with terrestrial electrons, the more difficult to detect ν_μ or ν_τ can be reconverted to the more easily detectable ν_e. The opposite process can also occur. The physics of this ''day-night'' effect is well understood [27]. We adopt the methodology of Ref. [28]. The SuperKamiokande Collaboration has placed constraints on neutrino oscillation parameters from the measurement of the zenith angle dependence in 504 days of data [8].

We first discuss in Sec. III A the day-night asymmetry averaged over all zenith angles and integrated over all energies and seasons of the year. We then analyze in Sec. III B the dependence of the total rate upon the solar zenith angle. We then describe in Sec. III C a new test, which we call the ''day-night'' spectrum test.

A. Integrated day-night effect

The average day-night asymmetry measured by the SuperKamiokande Collaboration is [15]

$$A_{\text{n-d}}=2\left[\frac{\text{night}-\text{day}}{\text{night}+\text{day}}\right]=0.060\pm 0.036(\text{stat})\pm 0.008(\text{syst}). \tag{4}$$

Here ''night'' (''day'') is the nighttime (daytime) signal averaged over energies above 6.5 MeV and averaged over all zenith angles and seasons of the year.[2]

Table II shows the calculated values for the day-night asymmetry for a range of different LMA solutions. For solutions within the allowed LMA domain, we find $A_{\text{n-d}}=0.02$–0.14.

The dependence of the asymmetry on Δm^2 can be approximated with the LMA solution space by

$$A_{\text{n-d}}=0.2\left[\frac{10^{-5}\ \text{eV}^2}{\Delta m^2}\right] \tag{5}$$

for $\sin^2 2\theta=0.8$ and for the range of Δm^2 shown in Table II.

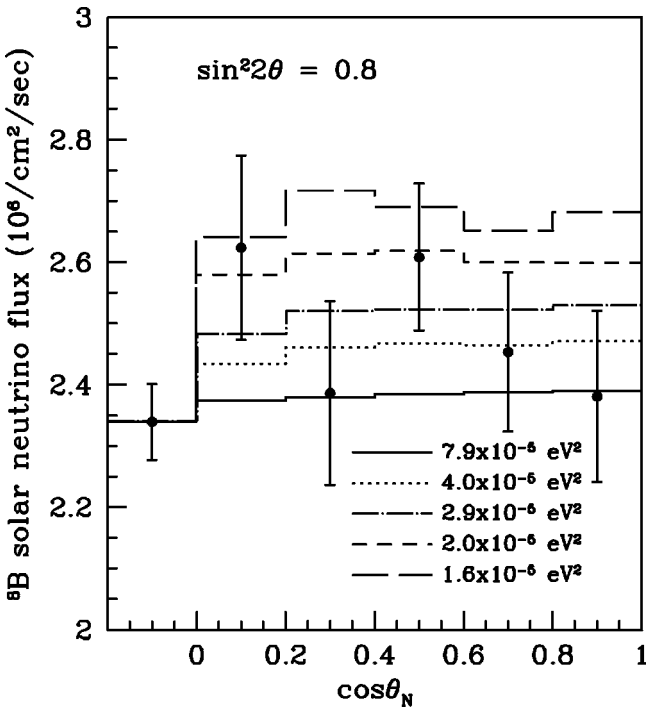

FIG. 4. The predicted versus the observed zenith angle dependence of the total event rate above 6.5 MeV. Here $\cos\Theta_N=\cos(\pi-\Theta)$, where Θ_N is the nadir angle and Θ is the zenith angle. The first bin is the average of the daytime rate of all of the observations. The figure shows the dependence of the ν-e scattering rate in the SuperKamiokande detector upon the nadir angle of the Sun at the time of the observation is shown for a representative range of Δm^2 and fixed $\sin^2 2\theta$. The results are averaged over an entire year. The data are from Ref. [9]. The calculational procedures are the same as in Ref. [28].

This approximation depends only weakly on mixing angle. The 1σ interval of $A_{\text{n-d}}$ that follows from Eq. (4) leads to an allowed range of

$$\Delta m^2=(2-8)\times 10^{-5}\ \text{eV}^2,\quad 1\sigma. \tag{6}$$

Figure 1 shows the approximately horizontal lines of equal night-day asymmetry in a Δm^2-$\sin^2 2\theta$ plot together with region in parameter space (dashed contour) that is allowed by a combined fit of the total rates and the night-day asymmetry. The best-fit oscillation parameters for the combined fit are

$$\Delta m^2=2.7\times 10^{-5}\ \text{eV}^2,\ \sin^2 2\theta=0.76. \tag{7}$$

The night-day asymmetry is 8% for these best fit parameters.

B. Zenith angle dependence

Figures 4 and 5 compare the predicted and the observed (after 708 days) dependence of the SuperKamiokande [9] event rate upon the zenith angle of the Sun, Θ. The results are averaged over 1 year. In order to make the figures look most similar to figures published by the SuperKamiokande Collaboration, we have constructed the plot using the nadir angle $\Theta_N=\pi-\Theta$. The predicted and the observed rates are averaged over all energies >6.5 MeV.

[1]If neutrino oscillations occur, the predicted zenith-angle dependence changes slightly for different solar models since the flavor content of the calculated solar flux arriving at Earth is influenced somewhat by the assumed standard model fluxes. See Ref. [28], Sec. X B.

[2]The definition of $A_{\text{n-d}}$ given in Eq. (4) is twice as large as in Ref. [28]; we changed our definition to the one given in the present paper in order to conform to the usage by the SuperKamiokande Collaboration. Similarly, we do not discuss the valuable constraints provide by moments of the day-night effect because the SuperKamiokande Collaboration has not yet provided an analysis of their results in terms of moments.

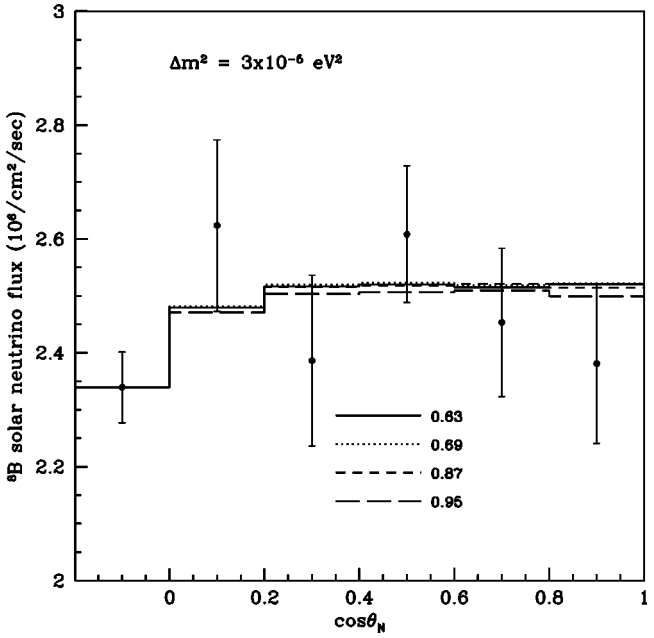

FIG. 5. For a fixed value of Δm^2 and a range of values of $\sin^2 2\theta$, the predicted versus the observed zenith angle dependence of the total event rate above 6.5 MeV. Same as Fig. 4 except for different oscillation parameters. This figure makes clear the difficulty of reducing the error bars so that they are smaller than the size of the predicted effect.

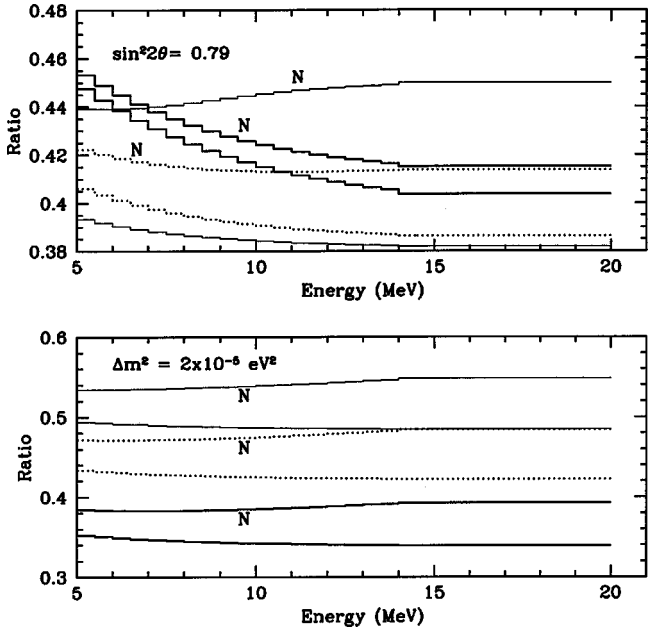

FIG. 6. The predicted day and night electron recoil energy spectra for a representative range of Δm^2 and $\sin^2 2\theta$. The night spectra are indicated on the figure by *N*; the corresponding day spectra are not marked. For the upper panel, the values of Δm^2 are (in units of 10^{-5} eV^2) 7.9 (thick solid line), 4.0 (dashed line), and 1.6 (thin solid line). For the lower panel, the values of $\sin^2 2\theta$ are 0.69 (thick solid line), 0.87 (dashed line), and 0.95 (thin solid line).

Three conclusions can be drawn from the results shown in Fig. 4 and Fig. 5. (1) The experimental error bars must be reduced by about a factor of 2 (total observation time of order 8 years) before one can make a severe test of the average zenith-angle distribution predicted by the LMA solution. (2) Nevertheless, the available experimental results provide a hint of an effect: all five of the nighttime rates are larger than the average rate during daytime. (3) The zenith-angle dependence predicted by the LMA solution is relatively flat; i.e., the flux is approximately the same for all zenith angles.

The predicted LMA enhancement begins in the first nighttime bin and the enhancement is not significantly increased when the neutrinos pass through the Earth's core [$\cos(\Theta) > 0.8$] and can even decrease for some parameter choices. As Δm^2 decreases, the oscillation length increases and the effect of averaging over oscillation phases becomes less effective with the result that some structure appears in the calculated zenith angle dependence. For $\Delta m^2 < 10^{-5}$ eV^2, the departure from a flat zenith angle dependence becomes relatively large.

Certain solutions of the SMA, those with $\sin^2 2\theta > 0.007$, predict a strong enhancement in the core that is not observed and therefore these SMA solutions are disfavored [9].

Figures 4 and 5 show that for $\Delta m^2 = (3-4)\times 10^{-5}$ eV^2 and a wide range of $\sin^2 2\theta$ the LMA solution provides an excellent fit to the zenith angle dependence.

The theoretical uncertainties [28] (due to the density distribution and composition of the Earth and the predicted fluxes of the standard solar model) are at the level of 0.2%, about an order of magnitude less than the effect that is hinted at by Fig. 4 and Fig. 5.

C. Day-night spectrum test

The spectral dependence of the day-night effect provides additional and independent information about neutrino properties that is not contained in the difference between the total day and the night event rates. The new physical information that is described by the difference between the day and the night energy spectra is the extent to which the different energies influence the total rates.

Figure 6 compares the calculated electron recoil energy spectra for the day and the night for a range of values of Δm^2 and $\sin^2 2\theta$. Again, we have plotted on the vertical axis of Fig. 6 the ratio, $R(E)$ [see Eq. (1)], of the measured recoil energy spectrum to the spectrum expected if there is no distortion.[3] The night spectra lie above the day spectra for all relevant energies. Moreover, the difference of the nighttime and the daytime rates increases with energy, reflecting the fact that for the LMA solutions the regeneration effect increases with Δm^2.

The systematic difference between the day and the night spectra is most easily isolated when the difference due to the

[3]The average energy spectra during the day and during the night have been calculated also in Ref. [29]. However, these authors did not include the SuperKamiokande energy resolution function, which leads to a significant smearing effect (see the discussions in Refs. [24,28,30]).

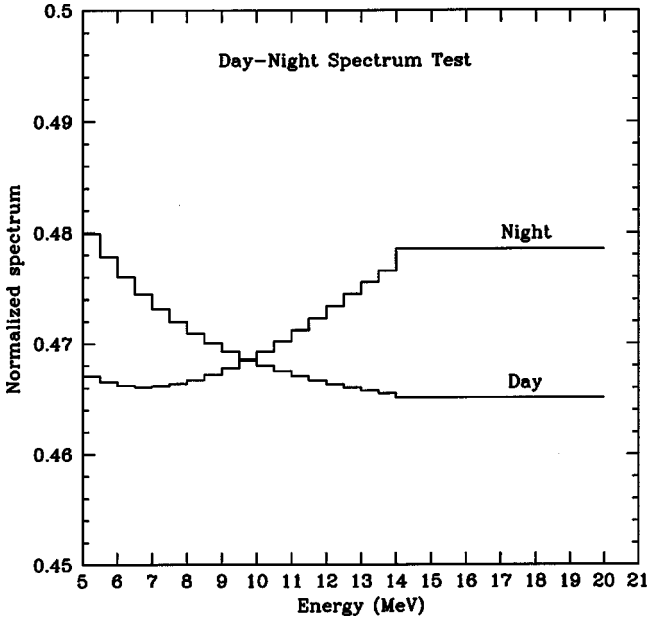

FIG. 7. The day-night spectrum test. The figure shows the characteristic difference between the recoil energy spectrum that is calculated for daytime observations and the energy spectrum that is calculated for nighttime observations. The particular curve that is shown in the figure was calculated for $\Delta m^2=2\times10^{-5}$ eV^2 and $\sin^2 2\theta=0.8$; similarly shaped curves are obtained for other LMA solutions with the same Δm^2 but different values of $\sin^2 2\theta$. The difference between the day and the night spectral shapes decreases as Δm^2 increases.

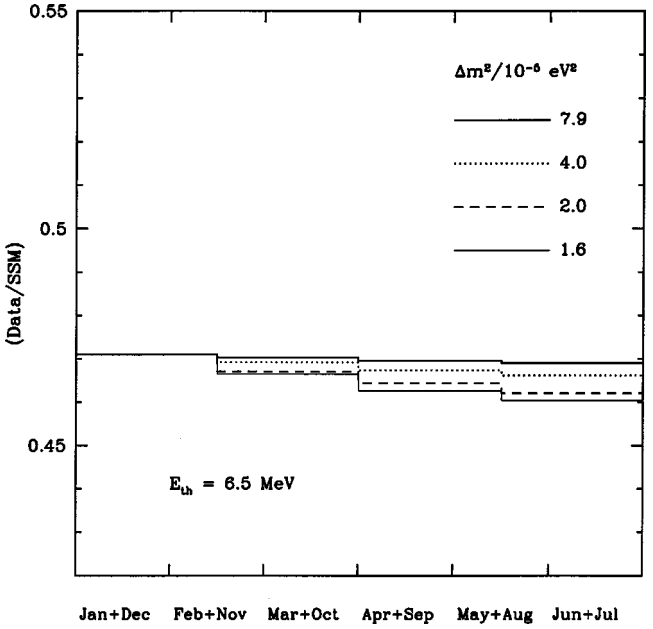

FIG. 8. The predicted seasonal dependence of the total event rate with eccentricity removed. The dependence of the ν-e scattering rate in the SuperKamiokande detector upon the season of the year is shown for a representative range of LMA solutions with variable Δm^2 and $\sin^2 2\theta=0.8$. In order to isolate the seasonal effect of neutrino oscillations, the effect of the eccentricity of the Earth's orbit has been removed. Figure 8 refers to all events above 6.5 MeV.

average rates is removed from both the day and the night spectra.

Figure 7 compares the daytime and the nighttime spectra when both spectra are normalized to the same total rate (the observed SuperKamiokande rate). This equal normalization removes the difference that is normally referred to as the ''day-night effect.'' We refer to the equal-normalization procedure as the ''day-night spectrum test.''

Figure 7 shows that for energies below (above) 10 MeV, the predicted differential daytime spectrum is higher (lower) than the predicted differential nighttime spectrum. The two normalized spectra become equal in rates at about 10 MeV. LMA predicts that the nighttime spectrum contains relatively more high energy electrons than the daytime spectrum.

Figure 7 shows that, when both spectra are normalized to have the same total rates, the average daytime spectrum between 5 MeV and 10 MeV is, for the parameters chosen, about $\sim$1.5% greater than the average nighttime spectrum. The oscillation parameters used to construct Fig. 7 are $\Delta m^2=2\times10^{-5}$ eV^2 and $\sin^2 2\theta=0.8$. We have plotted figures similar to Fig. 7 for a number of LMA solutions. For a fixed Δm^2, the equally normalized spectra are all very similar to each other. However, the amplitude of the difference between the night and the day spectra, about 3% at 5 MeV for the example shown in Fig. 7, decreases to about 2% for $\Delta m^2=4\times10^{-5}$ eV^2 and is only about 0.5% for $\Delta m^2=8\times10^{-5}$ eV^2.

Does the day-night spectrum test provide information independent of the information obtained from the integrated day-night rate effect or the more general zenith-angle effect? Yes, one can imagine that the day-night integrated effect (cf. Sec. III A) has been measured to be of order 6% in agreement with LMA predictions, but that when the day-night spectrum test is applied the appropriately normalized day rate at energies less than 10 MeV lies below the similarly normalized nighttime rate. This latter result would be inconsistent with the predictions of the LMA solution and therefore would provide information not available by just measuring the integrated difference of day and of night rates.

The easiest way to apply the day-night spectrum test is to normalize the day and night spectra to the same total number of events and then compare the number of day events below 10 MeV with the number of night events below 10 MeV In principle, one could divide the data into a number of different bins and test for the similarity to the predicted shape shown in Fig. 7, but Poisson fluctuations would dominate if the data were divided very finely.

The change in slope with energy, illustrated in Fig. 7, between equally normalized day and night recoil energy spectra may provide a new test of the LMA solution. It will also be useful to calculate the predicted change in slope for other solar neutrino solutions.

IV. SEASONAL DEPENDENCES

If the LMA solution is correct, seasonal dependences occur as a result of the same physics that gives rise to the zenith-angle dependence of the event rates. At nighttime, oscillations in matter can reconvert ν_μ or ν_τ to ν_e or matter

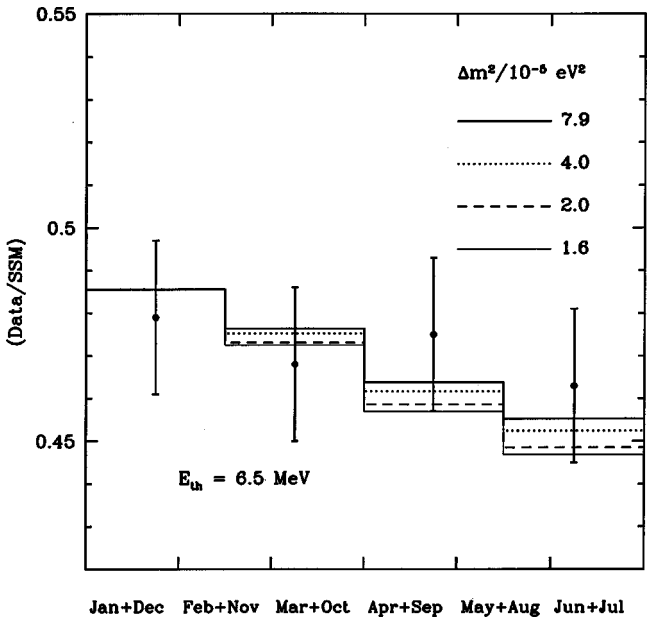

FIG. 9. The predicted seasonal plus eccentricity dependences of the total event rate. This figure is the same as Fig. 8 except that for the present figure we have not removed the effect of the eccentricity of the Earth's orbit in the predictions or the observations. The data are from Ref. [9].

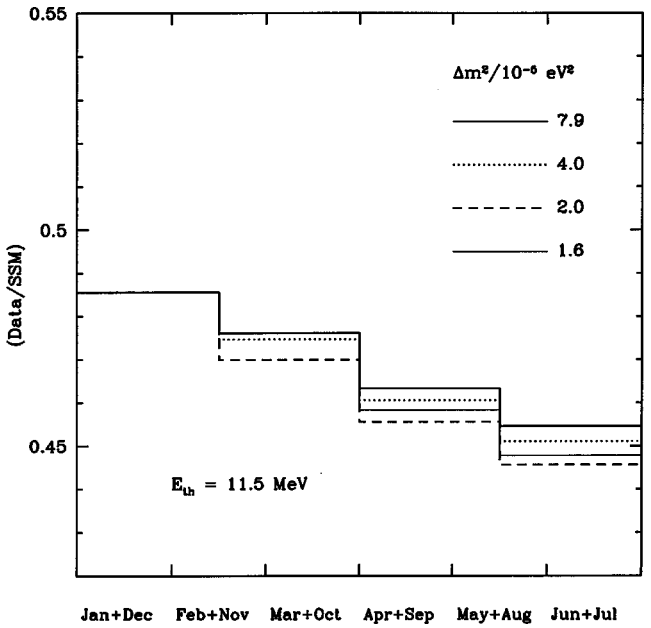

FIG. 10. The predicted seasonal plus eccentricity dependences of the total event rate for $E_{\rm th}=11.5$ MeV. This figure is the same as Fig. 9 except that the threshold recoil electron energy is larger.

interactions can also cause the inverse process. The seasonal dependence arises primarily because the night is longer in the winter than in the summer. Early discussions of the seasonal effect with applications to radiochemical detectors are given in Refs. [31]. A recent discussion of seasonal effects is presented in Ref. [32].[4]

A. Predicted versus observed seasonal dependence

Figures 8 and 9 show the predicted LMA variation of the total event rates as a function of the season of the year. In constructing Fig. 8, we corrected the counts for the effect of the eccentricity of the Earth's orbit. We show in Fig. 8 the predictions for a threshold of 6.5 MeV; Fig. 10 shows similar results for a threshold of 11.5 MeV. In both cases, the seasonal effects are small, $\sim 1\%-2\%$, although the higher-energy events exhibit a somewhat larger (30% or 40% larger) variation. The characteristic errors bars for SuperKamiokande measurements 3 years after beginning the operation are larger, typically $\sim 4\%$ (cf. Fig. 9), than the predicted LMA seasonal variations.

How do the SuperKamiokande data compare with the observations? For a threshold energy of 6.5 MeV, the data corrected for the Earth's eccentricity are not yet available. Therefore, we compare in Fig. 9 the observed [9] and the predicted seasonal plus eccentricity dependence. The eccentricity dependence is larger (for the allowed range of parameters) than the predicted LMA seasonal dependence; hence, the predicted variations in Fig. 9 are larger than in Fig. 8. The regeneration effect enhances the eccentricity effect in the northern hemisphere. In the southern hemisphere, the eccentricity and the regeneration-seasonal effects have opposite signs. This difference is in principle detectable; if the seasonal asymmetry is 7% in the northern hemisphere, then it would be about 3% in the southern hemisphere.

Unfortunately, the existing statistical error bars are too large to show evidence of either the eccentricity or the LMA seasonal dependence.

If the LMA solution is the correct description of solar neutrino propagation, it appears likely from Fig. 9 that an order of 10 years of SuperKamiokande data will be required in order to see a highly significant seasonal effect due to LMA neutrino mixing.

B. Relationship between the summer-winter and the day-night effect

Since the physics underlying the day-night and the seasonal dependences is the same, i.e., non-resonant matter mediated neutrino oscillations, there must be a relationship between the two effects. We outline here a brief derivation of a formula that connects the size of the day-night asymmetry defined in Eq. (4) and the winter-summer asymmetry, which we define as

$$A_{\rm W-S}\equiv 2\left(\frac{\text{winter}-\text{summer}}{\text{winter}+\text{summer}}\right). \tag{8}$$

Here ''winter'' (''Summer'') is the signal averaged over the period from November 15 to February 15 (May 15 to August 15).

[4]The principal results given in this section, including Eq. (10), have been presented and discussed by A. Yu. Smirnov at the Moriond meeting for 1999 [33]. The seasonal variations found in Ref. [32] are in good agreement with our results for the same values of the oscillation parameters.

TABLE III. LMA versus vacuum oscillations. Section III contains a quantitative discussion of the day-night integrated effect, the zenith angle dependence of the rate, and the day-night spectrum test. Seasonal effects are discussed in Sec. IV and spectrum distortion is discussed in Sec. II.

Phenomenon	LMA	Vacuum
Day-night integrated effect	Small but non-zero	Zero
Zenith-angle dependence of rate	Small but non-zero	Zero
Day-night spectrum test	Small but non-zero	Zero
Spectrum distortion	Flat relative spectrum	Can explain upturn at large energies
Seasonal effect	Eccentricity dominates	Can be large and energy dependent

Neutrinos reaching the Earth from the Sun will be in an incoherent mixture of mass eigenstates [34,35]. When the Sun is below the horizon, the presence of electrons in the Earth will cause some transitions to occur between different mass states. By solving the problem of matter induced neutrino transitions in a constant density medium, one can see that the characteristic oscillation length in the Earth is always less than or equal to the vacuum oscillation length divided by $\sin 2\theta$. The transition probability is proportional to $\sin^2(\phi)$, where

$$\phi \geqslant \frac{\pi R \sin 2\theta}{L_V} = 17 \sin 2\theta \left(\frac{R}{R_{\rm Earth}}\right)\left(\frac{10\ \ {\rm MeV}}{E}\right) \times \left(\frac{\Delta m^2}{2\times 10^{-5}\ \ {\rm eV}^2}\right), \tag{9}$$

where R is the distance traversed in the Earth. For any of the nighttime bins discussed in Sec. III, the phase of the oscillation is large so that even relatively small changes in distance and energy will lead to fast oscillatory behavior that causes the survival probability to average to a constant in all of the bins [cf. Eq. (9)]. This is the reason why the zenith-angle enhancement shown in Fig. 4 is approximately a constant, independent of zenith angle.

The event during the night and the event rate during the day are each approximately constant and may be represented as R_N and R_D, respectively. Let the average duration of night be t_S hours during the summer and t_W hours during the winter. Then the summer signal is proportional to $[R_N t_S + R_D(24-t_S)]$. There is a similar expression for the winter signal: $[R_N t_W + R_D(24-t_W)]$. Then simple algebra shows that the seasonal asymmetry is

$$A_{\rm W-S} = A_{\rm n\text{-}d}\left(\frac{t_W - t_S}{24}\right). \tag{10}$$

Thus the seasonal variations are proportional to the night-day asymmetry. The larger the day-night effect, the larger is the LMA predicted seasonal variations due to regeneration. For the location of SuperKamiokande, $t_W = 13.9$ h and $t_S = 10.1$ h, and the parenthetical expression in Eq. (10) is about 1/6.

Equation (10) gives the approximate relation between the seasonal and the day-night asymmetries and makes clear why the seasonal dependence is about 6 times smaller than the already small day-night effect. For the central value of the measured range of day-night asymmetries [15] [cf. Eq. (4)], we find from Eq (10) $A_{\rm W-S} \sim 1\%$, in agreement with our explicit calculations.

V. VACUUM VERSUS LMA OSCILLATIONS

Table III summarizes the most striking differences in the predictions of the LMA and the vacuum oscillation solutions of the solar neutrino problems. We now discuss some aspects of these differences in more detail.

The sharpest distinctions between vacuum and LMA predictions are expressed in the day-night differences. The LMA predicts non-zero day-night differences for all three of the tests discussed in Sec. III and listed as the first three phenomena in Table III. Vacuum oscillations predict zero for all these day-night phenomena.

The spectrum distortion is predicted to be small for the LMA solution (cf. Fig. 3). The ratio of the observed to the standard spectrum is essentially constant for energies above 6.5 MeV, although a modest upturn can occur at lower energies. Vacuum oscillations allow a more varied set of spectral distortions and can accommodate, without enhanced *hep* production, the possibly indicated upturn in the relative spectrum beyond 13 MeV.

One can use seasonal variations to distinguish between vacuum oscillations and LMA oscillations. For an early discussion of this possibility, see Ref. [36]. The LMA solution predicts that the seasonal effects are smaller than the geometrical effect arising from the eccentricity of the Earth's orbit. Moreover, there is only a weak enhancement of the LMA seasonal effect with increasing energy threshold. On the other hand, for vacuum oscillations the seasonal effects can be comparable with the geometrical effect and there can be a strong enhancement (or an almost complete suppression, even a reversal of the sign) of the seasonal effect as the threshold energy is increased (see first paper in Ref. [36]).

For the LMA solution, regeneration occurs but only during the night. Therefore, the LMA solution predicts that there is no seasonal dependence of the daytime signal beyond that expected from the eccentricity of the Earth's orbit. The vacuum oscillation solutions predict that the day and the night seasonal dependences will be the same. Therefore, in principle one could distinguish between vacuum oscillations and LMA oscillations by comparing the seasonal dependence observed during daytime with the seasonal dependence observed at night.

The LMA solution predicts for experiments measuring the

low energy ^{7}Be neutrino line (BOREXINO, KamLAND, LENS) that there will not be a significant contribution to the seasonal effect beyond that expected from the eccentricity of the Earth's orbit. This is because the day-night difference is very small at low energies in the LMA solution [28,12]. For vacuum oscillations, there can be significant seasonal dependences of the ^{7}Be line in addition to the purely geometrical effect .

SuperKamiokande data can be used to test for an enhancement of the seasonal variations as the energy threshold for selecting events is increased. Such an enhancement might be produced by vacuum oscillations. Vacuum oscillations with $\Delta m^2 \sim 4\times 10^{-10}$ eV^2, which give the best description of the recoil energy spectrum, provide a distinct pattern for the enhancement: the effect of eccentricity is larger than the effect of oscillations for a threshold energy of 6.5 MeV, while the effect of oscillations is comparable with the eccentricity effect for a threshold of 11.5 MeV [36].

Comparing Fig. 10 and Fig. 9, we see that the enhancement with energy threshold predicted by LMA is weaker than for vacuum oscillations. For LMA, the increase in the threshold only enhances the seasonal variations by an order of 30%–40% of an already small effect. This insensitivity to changes in energy threshold is in agreement with our calculations of the day and night recoil energy spectra (see Sec. IV B).

Practically speaking, LMA predicts for SuperKamiokande that there will be no measurable change in the seasonal effect with increasing energy threshold.

VI. SUMMARY AND DISCUSSION

A. Current situation

The large mixing angle solution is consistent with all the available data from solar neutrino experiments. Figure 1 shows the allowed region of the LMA parameters in the approximation of two oscillating neutrinos.

We have investigated in this paper the LMA predictions for SuperKamiokande of the distortion of the electron recoil energy spectrum, the integrated day-night effect, the zenith-angle dependence of the event rate, and the seasonal dependences. We have also evaluated and discussed an independent test, which we call the day-night spectrum test. Finally, we have analyzed the possibilities for distinguishing between LMA and vacuum oscillations (see Table III and the discussion in Sec. V). We previously showed that the LMA solution is globally consistent with the measured rates in the chlorine, Kamiokande, SAGE, GALLEX, and SuperKamiokande experiments [12].

The electron recoil energy spectrum predicted by the LMA solution is practically undistorted at energies above 7 MeV; i.e., the ν_e survival probability is essentially independent of energy at high energies. However, the recoil energy spectrum that is measured by SuperKamiokande suggests an increased rate, relative to the standard recoil energy spectrum, for energies above 13 MeV [5,6,8,9].

We have discussed in Sec. II B two experimental possibilities for explaining the upturn at large energies of the recoil energy spectrum: (1) a statistical fluctuation that will go away as the data base is increased and (2) an error in the absolute energy calibration. Figure 2 shows that a best fit to the upturn at large energies would require a several sigma error in the absolute energy calibration. Both of these seemingly unlikely possibilities, a large statistical fluctuation and a large error in the energy calibration, will be tested by future measurements with SuperKamiokande.

There are at least two possibilities for explaining the spectral upturn that do not involve experimental errors or statistical fluctuations: (1) a *hep* flux that is approximately 10–30 times larger than the conventional nuclear physics estimate and (2) vacuum oscillations. We have concentrated in this paper on the explanation that invokes a larger-than-standard *hep* flux. Our results are illustrated in Fig. 3. Even when the enhanced rate is used in the calculations, the *hep* neutrinos are so rare that they do not effect anything measurable except the energy spectrum.

At energies below 7 MeV, the LMA solution predicts a slight upturn in the recoil energy spectrum relative to the standard model energy spectrum. This effect is shown in Fig. 3 and may be detectable in the future with much improved statistics.

However, Fig. 2 shows that even a modest error in the absolute energy calibration could give rise to an apparently significant energy distortion. In future analyses, it will be important to include the absolute energy calibration error as one of the parameters that is allowed to vary in determining the best fit and the uncertainty in the spectrum shape.

The zenith-angle dependence and the integrated day-night effect observed by SuperKamiokande are consistent with the predictions of the LMA and, in fact, show a hint of an effect ($\sim 1.6\sigma$) that is predicted by LMA oscillations [see Ref. [15] and Eq. (4)]. Figures 4 and 5 show that the predicted and the observed nighttime enhancement are both relatively flat, approximately independent of the zenith angle. Moreover, all five of the measured nighttime rates are above the average daytime rate. However, the results are not very significant statistically. If the LMA description is correct, then another 5–10 years of SuperKamiokande data taking will be required in order to reveal a several standard deviation effect.

The difference between the daytime and the nighttime recoil energy spectra may be detectable in the future. Figure 6 shows separately the predicted day and the predicted night spectral energy distributions.

The most useful way to test for differences between the shapes of the daytime and the nighttime energy spectra is to normalize both spectra to the same value. Figure 7 shows the predicted difference between the spectra observed during the day and the spectra observed at night. It will be extremely interesting to test the hint that a day-night effect has been observed with SuperKamiokande by comparing, as in Fig. 7, the equally normalized day and night spectra. The simplest way of performing this test would be to compare the total area of the energy spectrum that is observed below 10 MeV at night with the total area observed below 10 MeV during the day. The predicted average difference in the day-night spectrum test is about 1.5% for $\Delta m^2 = 2\times 10^{-5}$ eV^2 and decreases to $\sim 0.5\%$ for $\Delta m^2 = 8\times 10^{-5}$ eV^2.

If the LMA solution is correct, then when the day and night spectra are normalized so that they have equal total areas, then the area under the daytime spectrum curve below 10 MeV must be larger than the area of the nighttime spectrum below 10 MeV. No significant difference between the daytime and the nighttime spectra is expected if vacuum oscillations are the correct solution of the solar neutrino problems.

Seasonal differences are predicted to be small for the LMA solution. Equation (10) shows that seasonal differences are expected to be reduced relative to the day-night asymmetry by a factor of the order of 6 for the location of SuperKamiokande, i.e., the difference between the average length of the night in the winter and the summer divided by 24 h. The predicted and the observed seasonal dependences are shown in Fig. 8 and Fig. 9. If the LMA solution is correct, it will require many years of SuperKamiokande measurements in order to detect a statistically significant seasonal dependence.

B. How will it all end?

If there is new physics in the neutrino sector, then experimentalists need to provide two different levels of evidence in order to ''solve'' the solar neutrino problems. First, measurements must be made that are inconsistent with standard electroweak theory at more than the 3σ level of significance. Second, diagnostic measurements must be made that uniquely select a single non-standard neutrino solution.

Where are we in this program?

We are much of the way toward completing the first requirement in a global sense. A number of authors have shown [12,37–39] that an arbitrary linear combination of fluxes from different solar nuclear reactions, each with an undistorted neutrino energy spectrum, is inconsistent at about 3σ or more with a global description of all of the available solar neutrino data. The data sets used in these calculations have gradually been expanded to include the results of all five solar neutrino experiments: Homestake, Kamiokande, SAGE, GALLEX, and SuperKamiokande. The results have become stronger as more data were added. The precise agreement [13] of the calculated sound speeds of the standard solar model with the measured helioseismological data has provided a further argument in support of the conclusion that some new physics is occurring.

However, we do not yet have a measurement of a smoking-gun phenomenon, seen in a single experiment, that is by itself significant at a many sigma level of significance. This has been the goal of the current generation of solar neutrino experiments.

What can we say about the possibility of achieving this goal with SuperKamiokande? There may of course be new physical phenomena that have not been anticipated theoretically and which will show up with a high level of significance in the SuperKamiokande experiment. We cannot say anything about this possibility.

If the LMA description of solar neutrinos is correct, we can use the results shown in Figs. 2 –10 to estimate how long SuperKamiokande must be operated in order to reduce the errors so that a single effect (spectrum distortion, zenith-angle dependence, or seasonal dependence) is significant at more than the 3σ level. Figures 2 –10 show that the errors must be reduced for any one phenomenon by at least a factor of two in order to reach a multi-sigma level of significance. Since the available data comprise 708 days of operation, over a calendar period of the order of 3 years, it seems likely that SuperKamiokande will require an order of a decade of running in order to isolate a single direct proof of solar neutrino oscillations, provided the LMA description is correct.

Fortunately, SuperKamiokande can make a global test of the standard electroweak hypothesis that nothing happens to neutrinos after they are created in the center of the Sun. This global test could become significant at the several sigma level within a few years even if the LMA solution is correct. For example, the combined effect of the zenith-angle dependence plus a possible spectral distortion at low energies might show up as a clear signal. Or both the integrated day-night effect and the day-night spectrum test could be observed. The combined statistical significance of several difference tests could be very powerful. With the great precision and the high statistical significance of the SuperKamiokande data, we think that there is a good chance that a many sigma result may be obtainable in a relatively few years.

Note added in proof. Recently, the SuperKamiokande Collaboration has made available the data for 825 days of observations (T. Kajita, talk given at the Second Int. Conf. ''Beyond the Desert,'' Castle Ringberg, Tegernsee, Germany, 1999). In this more complete data set, the significance of the excess of events at high energies has further decreased and the day-night asymmetry has increased to approximately the 2σ level. Both of these developments strengthen slightly the case for the LMA solution.

ACKNOWLEDGMENTS

We are grateful to the SuperKamiokande Collaboration for continuing to make available their superb preliminary data and for many stimulating discussions. We are also grateful to David Saxe for skillfully performing some numerical calculations. J.N.B. acknowledges support from NSF grant No. PHY95-13835 and P.I.K. acknowledges support from NSF grant No. PHY95-13835 and NSF grant No. PHY-9605140.

[1] B.T. Cleveland *et al.*, Astrophys. J. **496**, 505 (1998); B.T. Cleveland *et al.*, Nucl. Phys. B (Proc. Suppl.) **38**, 47 (1995); R. Davis, Prog. Part. Nucl. Phys. **32**, 13 (1994).

[2] KAMIOKANDE Collaboration, Y. Fukuda *et al.*, Phys. Rev. Lett. **77**, 1683 (1996).

[3] SAGE Collaboration, V. Gavrin *et al.*, in *Neutrino 96*, Proceedings of the XVII International Conference on Neutrino Physics and Astrophysics, Helsinki, edited by K. Huitu, K. Enqvist and J. Maalampi (World Scientific, Singapore, 1997), p. 14; J.N. Abdurashitov *et al.*, in *Neutrino 98*, Proceedings of

the XVIII International Conference on Neutrino Physics and Astrophysics, Takayama, Japan, 1998, edited by Y. Suzuki and Y. Totsuka [Nucl. Phys. B (Proc. Suppl.) **77**, 20 (1999)].
[4] GALLEX Collaboration, P. Anselmann *et al.*, Phys. Lett. B **342**, 440 (1995); GALLEX Collaboration, W. Hampel *et al.*, *ibid.* **388**, 364 (1996).
[5] SuperKamiokande Collaboration, Y. Fukuda *et al.*, Phys. Rev. Lett. **81**, 1158 (1998); **81**, 4279(E) (1998).
[6] SuperKamiokande Collaboration, Y. Suzuki, in *Neutrino 98* [4].
[7] SuperKamiokande Collaboration, Y. Fukuda *et al.*, Phys. Rev. Lett. **82**, 1810 (1999).
[8] SuperKamiokande Collaboration, Y. Fukuda *et al.*, Phys. Rev. Lett. **82**, 2430 (1999).
[9] SuperKamiokande Collaboration, M. Smy, Phys. Lett. B **456**, 204 (1999).
[10] Y. Suzuki, talk given at the 17th International Workshop on Weak Interactions and Neutrinos, Win-99, Cape Town, South Africa, 1999 (unpublished).
[11] H. Minakata and H. Nunokawa, Phys. Rev. D **59**, 073004 (1999).
[12] J.N. Bahcall, P.I. Krastev, and A.Yu. Smirnov, Phys. Rev. D **58**, 096016 (1998).
[13] J.N. Bahcall, S. Basu, and M.H. Pinsonneault, Phys. Lett. B **433**, 1 (1998).
[14] L. Wolfenstein, Phys. Rev. D **17**, 2369 (1978); S.P. Mikheyev and A.Yu. Smirnov, Yad. Fiz. **42**, 1441 (1985) [Sov. J. Nucl. Phys. **42**, 913 (1985)]; Nuovo Cimento C **9**, 17 (1986).
[15] K. Inoue, VIII International Workshop on ''Neutrino Telescopes'' Venice, 1999 (unpublished).
[16] Y. Fukuda *et al.*, Phys. Rev. Lett. **81**, 1562 (1998).
[17] O.L.G. Peres and A. Yu. Smirnov, Phys. Lett. B (to be published), hep-ph/9902312.
[18] J.N. Bahcall, E. Lisi, D.E. Alburger, L. De Braeckeleer, S.J. Freedman and J. Napolitano, Phys. Rev. C **54**, 411 (1996).
[19] J.N. Bahcall, Phys. Rev. D **44**, 1644 (1991).
[20] J.N. Bahcall, M. Kamionkowski, and A. Sirlin, Phys. Rev. D **51**, 6146 (1995).
[21] J.N. Bahcall and P. Krastev, Phys. Lett. B **436**, 243 (1998).
[22] R. Escribano, J.M. Frere, A. Gevaert, and D. Monderen, Phys. Lett. B **444**, 397 (1998).
[23] G. Fiorentini *et al.*, Phys. Lett. B **444**, 387 (1998).
[24] J.N. Bahcall and E. Lisi, Phys. Rev. D **54**, 5417 (1996); J.N. Bahcall, P.I. Krastev, and E. Lisi, Phys. Rev. C **55**, 494 (1997).
[25] Q. Y. Liu, talk given at the 17th International Workshop on Weak Interactions and Neutrinos, Cape Town, South Africa, 1999.
[26] E. Adelberger *et al.*, Rev. Mod. Phys. **70**, 1265 (1998).
[27] S.P. Mikheyev and A. Yu. Smirnov, in *'86 Massive Neutrinos in Astrophysics and in Particle Physics*, proceedings of the Sixth Moriond Workshop, edited by O. Fackler and Y. Trân Thanh Vân (Editions Frontières, Gif-sur-Yvette, 1986), p. 355; J. Bouchez *et al.*, Z. Phys. C **32**, 499 (1986); M. Cribier, W. Hampel, J. Rich, and D. Vignaud, Phys. Lett. B **182**, 89 (1986); M.L. Cherry and K. Lande, Phys. Rev. D **36**, 3571 (1987); S. Hiroi, H. Sakuma, T. Yanagida, and M. Yoshimura, Phys. Lett. B **198**, 403 (1987); S. Hiroi, H. Sakuma, T. Yanagida, and M. Yoshimura, Prog. Theor. Phys. **78**, 1428 (1987); A. Dar, A. Mann, Y. Melina, and D. Zajfman, Phys. Rev. D **35**, 3607 (1988); M. Spiro and D. Vignaud, Phys. Lett. B **242**, 279 (1990); A.J. Baltz and J. Weneser, Phys. Rev. D **35**, 528 (1987); A.J. Baltz and J. Weneser, *ibid.* **37**, 3364 (1988).
[28] J.N. Bahcall and P.I. Krastev, Phys. Rev. C **56**, 2839 (1997).
[29] M. Maris and S.T. Petcov, Phys. Rev. D **56**, 7444 (1997).
[30] A. Guth, L. Randall, and M. Serna, hep-ph/9903464.
[31] M. Cribier *et al.*, Phys. Lett. B **188**, 169 (1987); M.L. Cherry and K. Lande, Phys. Rev. D **36**, 3571 (1987); see also A.J. Baltz and J. Weneser, *ibid.* **35**, 528 (1987).
[32] P.C. de Holanda, C. Pena-Garay, M. C. Gonzalez-Garcia, and J. W. F. Valle, Phys. Rev. D (to be published) hep-ph/9903473.
[33] A. Yu. Smirnov, XXXIVth Recontres de Moriond, Electroweak Interactions and Unified Theories, Les Arcs, 1999; S. P. Mikheyev and A. Yu. Smirnov, in *New and Exotic Phenomena*, Proceedings of 7th Moriond Workshop, edited by O. Fackler and J. Tran Thanh Van (Editions Frontiéres, Gif-sur-yvette, 1987), p. 403; in *Neutrinos*, edited by H. V. Klapdor (Springer-Verlag, Berlin, 1987), p. 239; see viewgraphs available at http://www.lal.in2p3.fr/CONF/Moriond
[34] A. Dighe, Q.Y. Liu, and A.Yu. Smirnov, hep-ph/9903329 1999.
[35] L. Stodolsky, Phys. Rev. D **58**, 036006 (1998).
[36] P.I. Krastev and S.T. Petcov, Nucl. Phys. B **449**, 605 (1995); S.P. Mikheyev and A.Yu. Smirnov, Phys. Lett. B **429**, 343 (1998); S.L. Glashow, P.J. Kernan, and L. Krauss, *ibid.* **445**, 412 (1999); V. Barger and K. Whisnant, Phys. Rev. D **59**, 093007 (1999); Phys. Lett. B **456**, 54 (1999); M. Maris and S.T. Petcov, *ibid.* **457**, 319 (1999); V. Berezinsky, G. Fiorentini and M. Lissia, hep-ph/9904225.
[37] N. Hata, S. Bludman, and P. Langacker, Phys. Rev. D **49**, 3622 (1994).
[38] S. Parke, Phys. Rev. Lett. **74**, 839 (1995).
[39] K.M. Heeger and R.G.H. Robertson, Phys. Rev. Lett. **77**, 3720 (1996).